Development of Simulation Based Liver and Spleen Injury Risk Curves for the GHBMC Detailed Models

Philippe Beillas, Fabien Berthet

Abstract This study investigated the ability of the GHBMC detailed female (F05) and male (M50) Finite Element models to predict abdominal solid organ injuries observed in Post Mortem Human Surrogate tests. Using 19 loading configurations from the literature corresponding to 68 Post Mortem Human Surrogate and a database of 173 simulations, simulation-based injury risk curves were developed for the liver and spleen of the GHBMC M50 and F05 models. A good or fair injury prediction capability (in the ISO rating sense) was attained for the liver when selecting carefully the loading condition based on the organ engagement. No equivalent result could be obtained on the spleen, most likely due to the insufficient number of injury points. The study highlights the critical importance of organ geometry and loading location to predict injury, and the limited effect of global model scaling on the injury prediction capability.

Keywords abdomen, human body model, injury, liver, risk curve

I. INTRODUCTION

Full body Finite Element Human Body Models (FE-HBMs) have the potential to predict injuries to abdominal solid organs such as the liver and spleen, but selecting a tolerance or developing a risk curve can be challenging. While tissue failure has been characterised in sample or isolated organ tests, it is not clear that it can be used directly *in situ* in a HBM due to (1) initial strain and pressure differences, e.g. [1] and (2) limitations of the HBM internal/local validation (as discussed in [2]). Full body assessment seem therefore critical to assess the injury prediction capability of FE-HBMs.

Full body Post Mortem Human Surrogate (PMHS) tests are typically used to assess the response of FE HBM. These tests also provide indications about soft organ injuries. However, anatomical organ positions and shapes are known to vary between subjects, e.g. [3-5]-, and experimental conditions including the lack of muscle tone in PMHSs could also affect the organ position (as hypothesised in [6]). The exact positions of the organ are typically not documented in PMHS tests, and a single FE HBM describes only a specific organ anatomy. The effects of a possible mismatch on organ loading were recently investigated and found to be significant.

In [2], impacts delivered to PMHS at various relative positions between liver and impactor were simulated with the Global Human Body Model Consortium, LLC (GHBMC) male 50th percentile (M50) detailed model scaled by morphing to the PMHS characteristics. The organ engagement by the impactor (characterised by the distance between liver and impactor) affected widely the average strain energy density (SED) in the liver. In [7], 15 loading conditions were applied to the GHBMC M50 and to the GHBMC F05 (5th percentile female) detailed models. The two models use similar modelling assumptions, i.e., the same material properties, element type, contact modelling, etc. Their main difference is their geometry that is based on different datasets. The simulations were performed on the baseline models, or on the models scaled by morphing to the estimated dimensions of each reference PMHS. Scaling improved the overall match between test and simulation responses. For example, scaling the models lead to an increase of the average CORA size score (CORA software version 3.61, Partnership for Dummies and Biomechanics, Germany) from 0.69 to 0.75 for the force and 0.51 to 0.61 for the deflection ($p<10^{-7}$). Scaling did not however affect the compression metric (deflection normalized by the depth, $p>0.25$). Peak data also reflected this effect. For example, scaling improved the experimental variance explained by the F05 simulations from $R^2=0.39$ to $R^2=0.61$ for the deflection, and from $R^2=0.76$ to $R^2=0.84$ for the force. For upper abdominal or distributed loading, the ratio between the SED in the F05 and M50 models scaled to the same PMHS dimensions was close to one, as could be expected considering the similarities of the models. However, the ratio

Philippe Beillas is a Researcher in Biomechanics at LBMC Ifsttar Université Lyon 1 in Bron, France (philippe.beillas@ifsttar.fr, +33472142371). Fabien Berthet is a Simulation Engineer at Transpolis SAS in Lyon Saint-Exupéry Aéroport, France.

was larger than two in the 10 setups (35 PMHSs) corresponding to mid abdomen loading with bars or belts. Similar trends were observed for the spleen with ratios at three or more for the same mid-abdomen loading. This higher SED in the F05 was attributed to a combination of organ shape and impact location: as the liver of the F05 is more caudal than the M50 (and its spleen more anterior), mid abdomen bar or belt loading engaged the F05 liver but was just below the M50 liver. Such sensitivity may substantially affect the ability to predict injury with the models, but the injury prediction capability was not assessed in [7].

The objectives of this study were therefore to (1) investigate the ability of the GHBMC detailed models to predict solid organ injuries based on 20 loading configurations from the literature and (2) build risk curves based on the results of the simulations. More specifically, risk curves will be built by combining the injury outcome of the PMHS tests with corresponding full body model predictions for the same organs. The curves are hence built using the models and do not directly use tissue or organ level tolerance data. The curves are therefore expected to be model and simulation specific. They will be referred to as simulation-based risk curves. For the analysis, the loading configurations were clustered to account for the sensitivity of SED to impact location.

II. METHODS

Loading Configurations and Simulation Database

Nineteen loading configurations corresponding to tests on 68 PMHS were used for the current study. They include impactor and belt loading, as well as side impact sleds. The peak SED in the liver, spleen or kidneys was used as injury criterion. Peak SED was selected as it was previously used to as an injury criterion for isolated organs [8] and is easy to compute at the organ level after a simulation. It was computed as the ratio between the internal energy in the organ and the initial organ volume. When not available in a study, an AIS level was assigned to each solid organ based on the injury description. There was no discrimination between male or female subjects in the experimental dataset, i.e. both were used independently of the gender of the model. Three approaches (called C1 to C3) were investigated for injury prediction:

- *C1 – Minimum SED in any test with AIS2+ organ injury*
- *C2 – Model-based AIS2+ risk curve based on all loading configurations*, not accounting for possible effects of SED sensitivity to the impact location and anatomy.
- *C3 – Model-based AIS2+ risk curve based on loading configurations for which the organ involvement is known.* The idea is to build a risk curve avoiding cases (loading configurations and models) for which the engagement of an organ of interest is uncertain. Based on [7], all mid-abdomen impactor and belt loading were excluded as it is unknown if these can consistently involve the liver and spleen due to variations of rib coverage, subject dimensions and organ locations. Configurations loading the upper abdomen, with distributed loading, e.g., side impact sleds, or for which the organ location is known [2] were kept.

The main loading locations and relative positions to the M50 and F05 organs are illustrated Fig. 1.

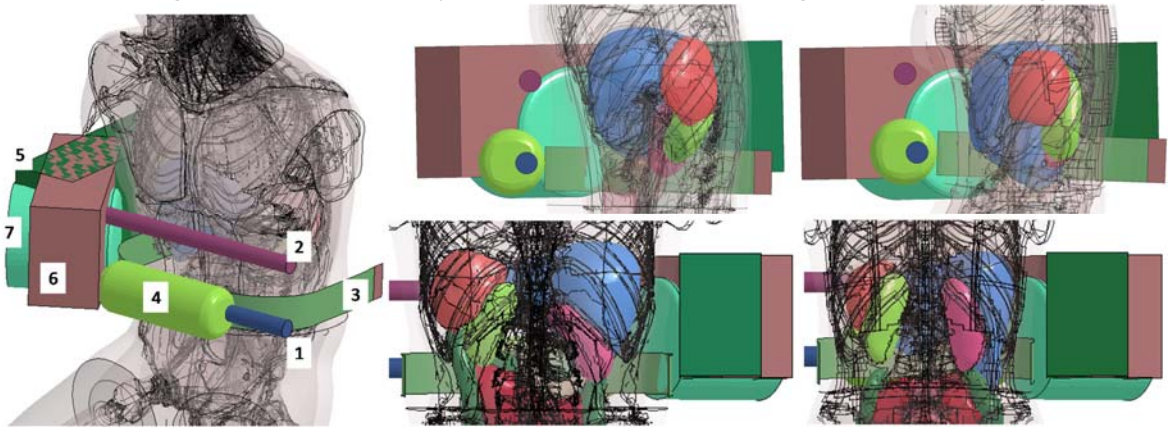

Fig. 1. Anatomical differences between models and possible effect on organ engagement. Left: loading setups (sleds not shown; mid (1) and upper (2) abdomen bar; mid abdomen belt (3); airbag surrogate (4); lateral (5) and oblique (6, 7) upper abdomen wide impactors). Middle: M50. Right: F05. For the F05, notice the lower position of the liver (in blue) and the more anterior position of the spleen (in red) than the M50. Configurations in positions similar to 1, 3 and 4 were not used for C3.

Three published detailed occupant models from the GHBMC were used for the current study: the male M50v4.3, and the female F05 v2.2 and v2.3. The solid organs of the F05 v2.2 and v2.3 are identical. All three models share the same modelling principles for the solid organs (tetrahedral solid mesh, capsule shell, a few major vessels as shells surrounding AIRBAG_LINEAR_FLUID for the contents). All models use exactly the same material properties. These are non-linear for the solid mesh (MAT_SIMPLIFIED_RUBBER for the liver, MAT_VISCOUS_FOAM for the spleen) and their surrounding capsules are elastic. Failure is not modelled. Organs are integrated in the cavity through attachments (e.g. falciform ligament, vessels) as well as sliding or tied contacts (e.g. bare area of liver). TABLE I summarises the configurations used for the current study and their C3 status selection. The C2 sample includes 24 liver, 11 spleen and 2 kidney AIS2+ injuries for 68 PMHSs while the C3 sample includes 10 liver, 4 spleen and 1 kidney AIS2+ injuries for 30 PMHSs.

Simulations were run with baseline models or after scaling to match the height, mass, and abdominal depth of specific PMHSs (as described in [2] and [7]). Simulations with scaled models corresponding to 60 PMHSs were run with the F05 v2.2 and M50 v4.3, using the exact stimulus used with the PMHSs (e.g. velocity). By exact stimulus, it is meant that the exact input condition (e.g. initial velocity) measured in a PMHS test was used with the corresponding scaled model. Input conditions used for all configurations are summarized in [2][7] and Appendix. Simulations with baseline models were run with the average stimulus. As the simulations were run during the F05 development phase, baseline simulations were also run with an updated F05 version (2.3). As not all simulations were run with all versions, TABLE I provides a summary of the 173 simulations used for the analysis. For most setups, the model responses, e.g., force, displacement, are summarised in [2] and [7] and will not be repeated here. Only the side impact sleds from [9], which are not previously described, are summarised in the Appendix.

Injuries and Risk Curve Calculation

C2 and C3 AIS2+ risk curves were calculated for liver and spleen using the principles of ISO TS18506. The process was automated using R scripts provided as Related Electronic Documents (version without age) [17], and Scilab for the plotting. The reported kidney injuries (only 2, TABLE I) was not sufficient to build risk curves.

To summarise the process, risk curves were built using survival analysis and the best fitting distribution among Weibull, log log or log normal. The best fit was selected using the AIC score. The risk curves were rated based on the width of the 95th percentile confidence interval divided by the risk (RR). Values of RR below 0.5 correspond to a good rating, values between 0.5 and 1 to a fair rating, values between 1 and 1.5 to a marginal rating and values above 1.5 to unacceptable. It was assumed that there is a single loading mechanism (compression of the organ). We did not check for overly influential points. Each PMHS was considered as a point for injury risk curve calculation. All points were considered as censored (left or right depending on the injury status) and:

- For scaled models: each simulation provides a SED value to which the injury status of the corresponding PMHS is associated.
- For baseline models: for a study with n PMHSs and n_i injured PMHSs, since there is only one SED value, it is used n_i times for injury points and n-n_i times for non-injury points to allow weighting studies.

TABLE I:

LOADING CONFIGURATIONS AND SIMULATIONS USED FOR THE F05 V22 (SCALED OR BASELINE), F05 V23 (BASELINE ONLY) AND M50V43 (SCALED OR BASELINE). EACH LINE MAY REPRESENT SEVERAL CONFIGURATIONS WITH FOR EXAMPLE DIFFERENT LOADING VELOCITIES (SEE N CONFIG). UNLESS OTHERWISE NOTED, EACH CONFIGURATION WAS SIMULATED USING THE M50V43, F05V22 AND F05V23 MODELS WITHOUT SCALING (THREE BASELINE RUN PER CONFIGURATION). EACH PMHS TEST WAS ALSO SIMULATED WITH THE F05V22 AND M50V43 SCALED TO THE DIMENSIONS OF THE PMHS (TWO SCALED RUNS PER PMHS). FOR EXAMPLE, THE FIRST LINE CORRESPONDS TO THREE CONFIGURATIONS (A, B AND C, I.E. 3X3=9 BASELINE RUNS) AND ELEVEN PMHS (2X11=22 SCALED RUNS). SEE TEXT FOR DEFINITION OF C3

Loading Configurations	N config.	nPMHS AIS2+	nPMHS used	Comment	Simulations available	Used C3
Cavanaugh bar mid abdo. A, B and C [9]	3	Liver: 2 Spleen: 1	11	Few injuries despite similarity to Hardy bar	Baselines (n=9) Scaled (n=22)	N
Foster pretensioner A and B [11]	2	Liver: 3 Spleen: 1	7	Only A condition has injuries	Baselines (n=6) Scaled (n=14)	N
Hallman side airbag [12]	1	Spleen: 1 Kidney: 1	2[a]		Baselines (n=3) Scaled (n=4)	Y
Hardy bar mid-abdo. (6 & 9 m/s) [13]	2	Liver: 5 Spleen: 2	6	Many injuries despite similarity to Cavanaugh	Baselines (n=6) Scaled (n=12)	N
Hardy bar to upper abdo. [13]	1	Liver: 3 Spleen: 1	3		Baselines (n=3) Scaled (n=6)	Y
Hardy Airbag surrogate [13]	1	Liver: 2	3		Baselines (n=3) Scaled (n=6)	N
Hardy belt [13]	1		3		Baselines (n=3) Scaled (n=6)	N
Kremer lateral [14]	1	Liver: 2	5	Less injuries than Kremer oblique	Baselines (n=3) Scaled (n=10)	Y
Kremer oblique [14]	1	Liver: 5	5	Many injuries despite similarity to Viano)	Baselines (n=3) Scaled (n=10)	Y
Lamielle MHA and PRT[b] [15]	2	Liver: 2 Spleen: 3 Kidney: 1	8		Baselines (n=6) Scaled (n=16)	N
Viano oblique [16]	1		4	No injuries despite similarity to Kremer oblique	Baselines (n=3) Scaled (n=8)	Y
Cavanaugh side sled soft & hard padding [9]	2	Spleen: 2	8		Baselines (n=4, F05v23, M50v43)	Y
Le Ruyet spherical impactor [2]	1		3[c]	Max SED of all impact locations	Scaled (n=6)	Y
	19 (C3: 7)	Liver: 24 (C3: 10) Spleen: 11 (C3: 4) Kidney: 2 (C3: 1)	68 (C3: 30)			

[a]Two PMHSs excluded (one with multiple impacts, one without spleen)

[b]MHA and PRT correspond to two belt loading configurations with different velocities. See [15] for details.

[c]Since there was multiple loading in several locations, only non-injury cases were used.

III. RESULTS

Minimum SED by Configuration and Model (C1)

Minimum SED obtained in simulations corresponding to injurious tests (C1) are reported in TABLE II. Almost all min SED values, i.e., for all organs and all models, were obtained for the same study, i.e., Lamielle belt loading, the only exception being for the spleen of the scaled F05 models (Hardy upper abdomen impact). For both liver and spleen, the SED was similar for scaled and baseline models (whether M50 or F05) and consistently smaller for the M50 than the F05. In order to check if the difference between the two models were only for the minimum value, cumulative plots of SED obtained in simulations corresponding to injurious tests are shown in Fig. 2. The plots confirm that the difference between the F05 and the M50 is present over most of the simulation set (the difference reduces for the highest SED) and for both baseline and scaled models.

TABLE II

MINIMUM SED VALUE OBSERVED IN A SIMULATION CORRESPONDING TO AN INJURIOUS TEST (SETUP IN PARENTHESIS). FOR THE KIDNEYS, THE RESULTS OF THE ONLY TWO INJURIOUS TESTS ARE PROVIDED.

Organ	Model (number of simulations)	Min SED (µJ/mm3)
Liver	F05 v2.3 baseline (N=19)	2.56 (Lamielle MHA)
	F05 v2.2 baseline(N=16)	2.45 (Lamielle MHA)
	Scaled F05 models (N=60)	2.52 (Lamielle MHA)
	M50 baseline (N=19)	0.72 (Lamielle MHA)
	M50 scaled (N=60)	0.86 (Lamielle MHA)
Spleen	F05 v2.3 baseline (N=19)	2.19 (Lamielle MHA)
	F05 v2.2 baseline (N=16)	2.45 (Lamielle MHA)
	Scaled F05 models (N=60)	2.79 (Hardy 7 up)
	M50 baseline (N=19)	0.55 (Lamielle MHA)
	M50 scaled (N=60)	0.70 (Lamielle MHA)
Kidneys	F05 v2.3 baseline (N=19)	6.17 (Lamielle PRT) - 12.1 (Hallman)
	F05 v2.2 baseline (N=16)	6.20 (Lamielle PRT) - 11.3 (Hallman)
	Scaled F05 models (N=60)	3.26 (Lamielle PRT) - 16.7 (Hallman)
	M50 baseline (N=19)	2.53 (Lamielle PRT) - 15.0 (Hallman)
	M50 scaled (N=60)	2.24 (Lamielle PRT) - 18.8 (Hallman)

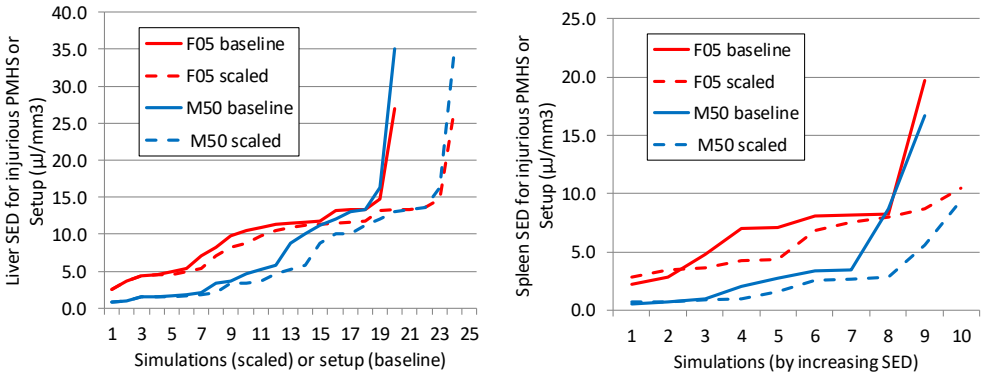

Fig. 2. Liver and Spleen peak SED for the simulations associated with injuries ranked by increasing value. The first value of each curve is reported in TABLE II.

Risk Curves using all Loading Configurations (C2)

The risk curves obtained for paired simulations (57 PMHSs) using baseline and scaled models were very similar (Fig. 3), with noticeable differences only visible for the C2 M50 liver. However, they differed widely between F05 and M50, and between organs. The best rating (fair or marginal) was just below 50% risk for the F05 liver, with corresponding SED almost identical for the baseline (10.04μJ/mm^3) and scaled (10.01μJ/mm^3) models. The C2 M50 liver curve had an unacceptable rating (RR around 2.5 around 40% risk), with corresponding SED around 4μJ/mm^3 for both scaled and baseline models. The C2 M50 liver risk curve predicted a 10% risk from almost no stimulus. For the spleen, the ratings were even lower. It was marginal at best around 20% risk for the baseline C2 F05 spleen (at 20%: RR=1.4, SED=5.6 μJ/mm^3). The SED value at 20% was similar (5.3 μJ/mm^3) for scaled F05 models despite a rating slightly above the unacceptable limit (RR=1.6). The M50 C2 Spleen curve had unacceptable rating with much higher RR (minimum RR of 2.7 for baseline and 7.9 for scaled models, both just below 20% risk). The M50 C2 Spleen predictions were similar for baseline and scaled models below 4 μJ/mm^3 or 20% risk, which covered most of the observations made in the simulations. Overall, while the global scaling approach reduced the difference between models and PMHSs, and also between models, it did not improve the risk predictions and did not reduce the differences between M50 and F05 (despite the two baseline models being very different in size).

In the following step, all configurations and PMHSs (n=68) were used by adding Cavanaugh sleds and scaled Le Ruyet results to the baseline runs. The effect on the risk curves was marginal (Fig. 4 vs. Fig. 3), and essentially limited to regions for which the confidence was small.

Risk Curves using Selected Loading Configurations (C3)

For the liver, as for C2, the C3 risk curves obtained for baseline and scaled models in paired simulations (Cavanaugh sleds and Le Ruyet excluded) were very similar (Fig. 5). However, the curve ratings were widely improved: near 50% risk, it was close to good for the F05 (RR=0.54) and fair for the M50 (RR=0.87). When using all C3 conditions (Fig. 6), the ratings were further improved. For the F05, the rating was good near 50% (RR=0.44) with a Liver SED of 12.7 μJ/mm^3. The minimum RR was 0.42 at 41.5% risk. For the M50, the rating was fair near 50% (RR=0.58) with a liver SED of 10.8 μJ/mm^3. The minimum RR was 0.57 at 44.9% risk. The use of C3 configurations (vs. all configurations) also had a tendency to reduce the difference in the shape of the risk curve between the M50 and F05 (Fig. 7). The C3 SED difference between F05 and M50 was 18% at 50% risk, with the value decreasing for higher risks while the C2 risk curves were diverging before.

For the spleen, the paired baseline and scaled risk curves were not plotted, as there were only two injuries in the C3 sample for scaled models. When using all C3 setups (including Cavanaugh sleds with two spleen injuries), the C3 ratings remained unacceptable as for the C2 curves (Fig. 6). For the F05, the minimum RR were just above the 1.5 unacceptable limit for both C2 and C3 F05 (1.6 at 23% risk for C3, 1.5 at 18% for C2) and the SED at 20% risk was higher for C3 (9 μJ/mm^3) than C2 (6.3 μJ/mm^3). For the M50, while remaining unacceptable, the minimum RR was improved for C3 (2.2 at 20% risk) over C2 (3.5 at 16.9% risk) and the SED at 20% risk was also higher for C3 (6.8 μJ/mm^3) than C2 (3.1 μJ/mm^3).

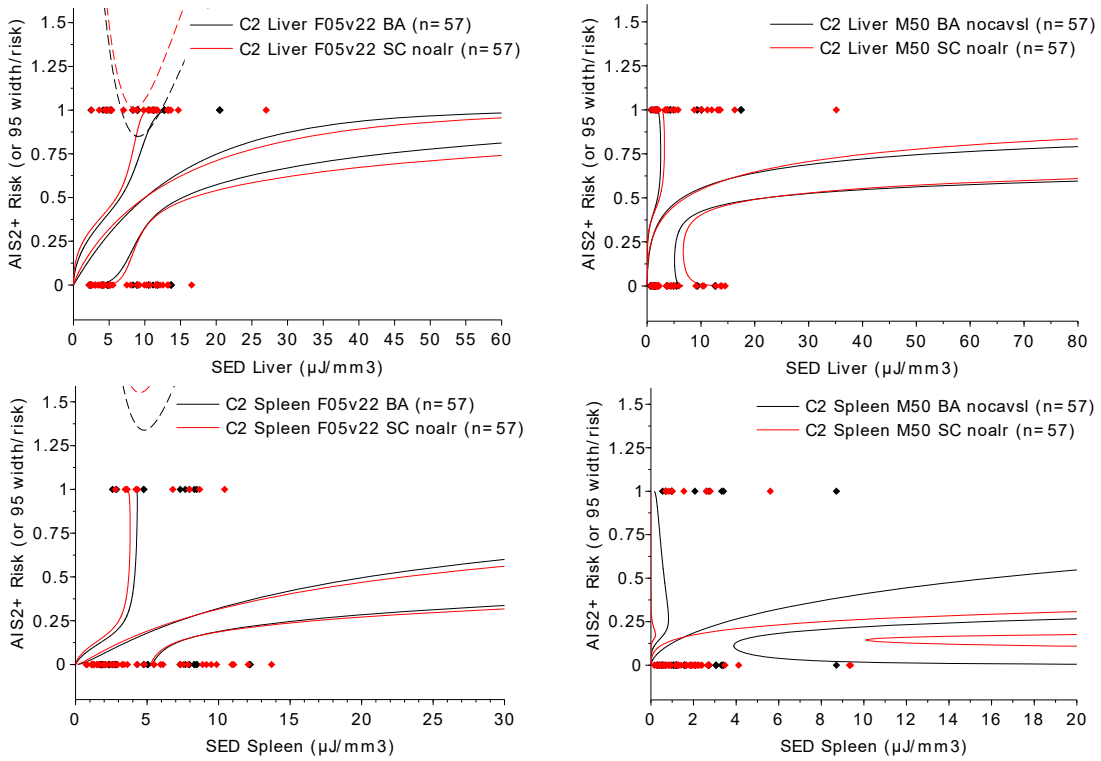

Fig. 3. Risk curves for baseline (black) and scaled (red) models (M50 and F05) using paired C2 simulations (baseline Cavanaugh Sled and scaled Le Ruyet excluded). Solid curves represent the average and 95th percentile interval, dashed curves the RR (rating: good<0.5, 0.5<fair<1, 1<marginal<1.5, 1.5<unacceptable). The squares are the injury points and *n* the number of PMHS considered (here: 57). BA=Baseline; SC=Scaled.

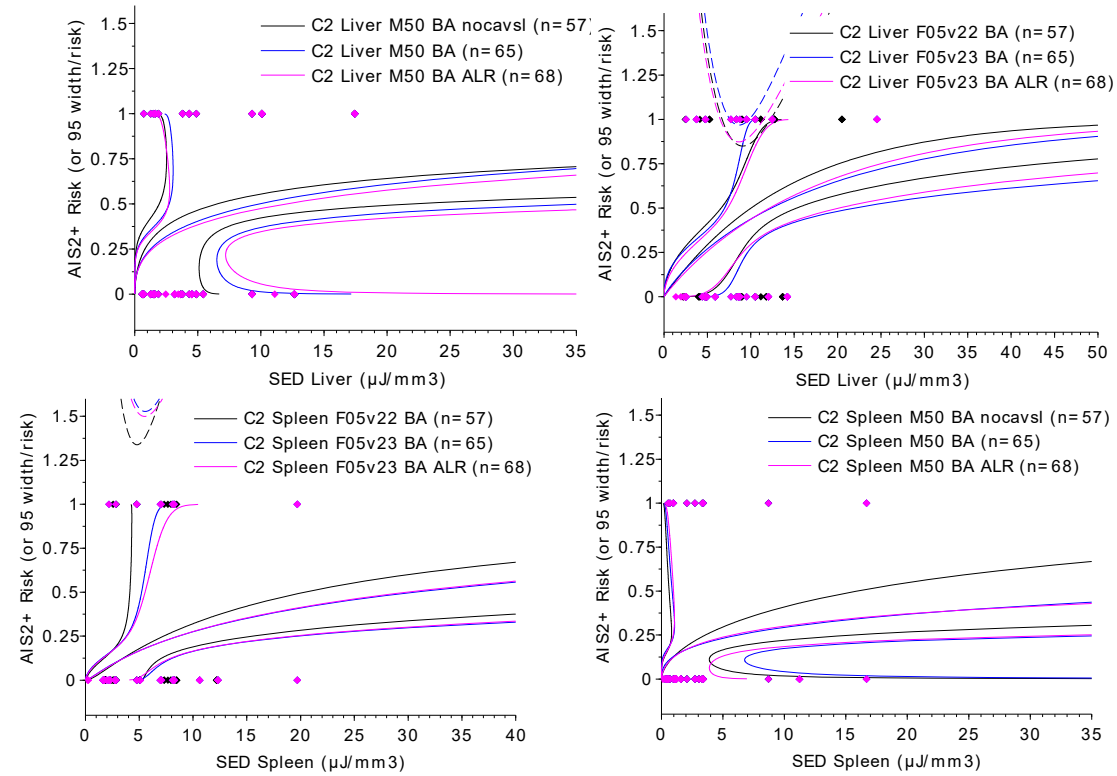

Fig. 4. C2 Risk curves using all configurations. Compared to Fig. 3 baseline (in back), Cavanaugh sleds (n=65) and Le Ruyet impacts (scaled models, n=68) were added. F05 was updated to v2.3. Legends as in Fig. 3.

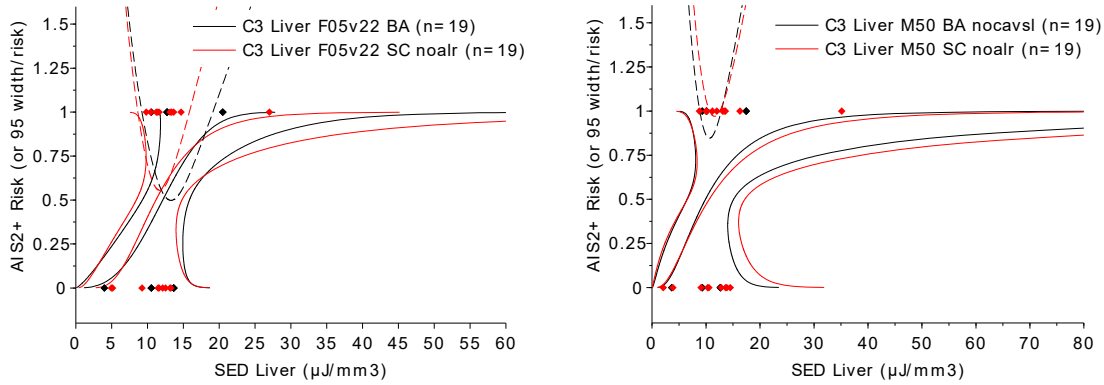

Fig. 5. Risk curves for baseline (black) and scaled (red) models (M50 and F05) using paired simulations from C3 (baseline Cavanaugh Sled and scaled Le Ruyet excluded). Legends as in Fig. 3.

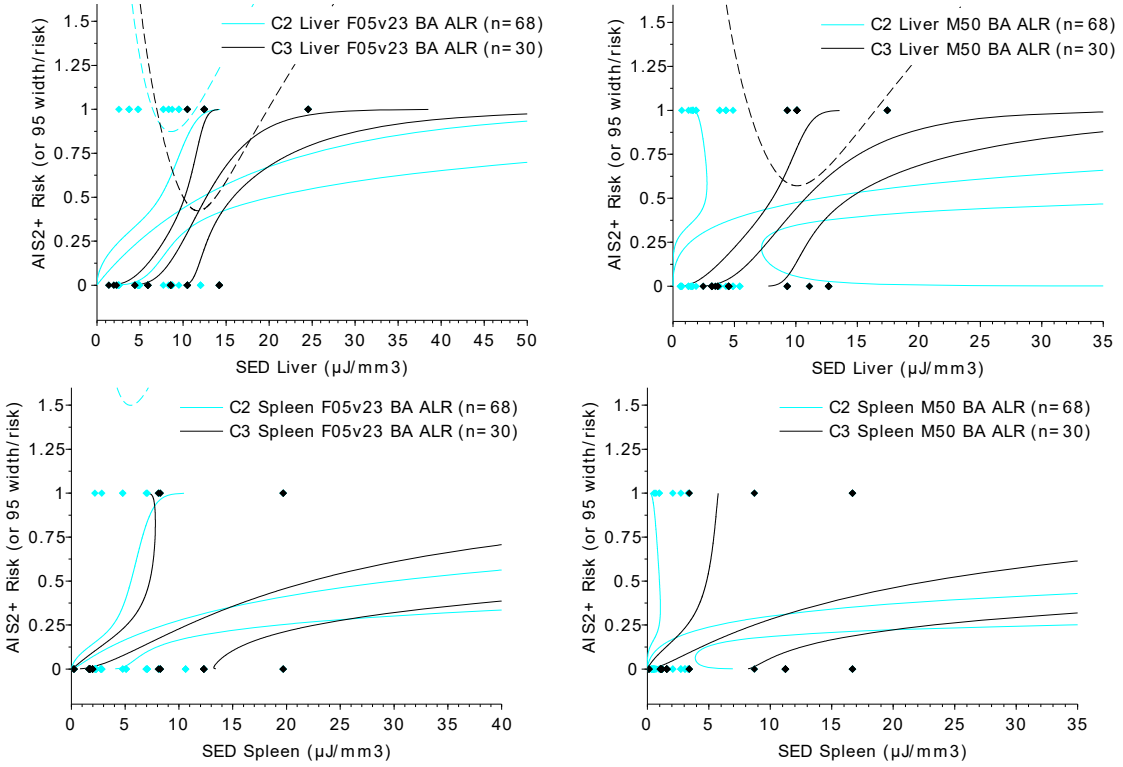

Fig. 6. Comparison of C3 and C2 risk curves (all configurations used). Legends as in Fig. 3.

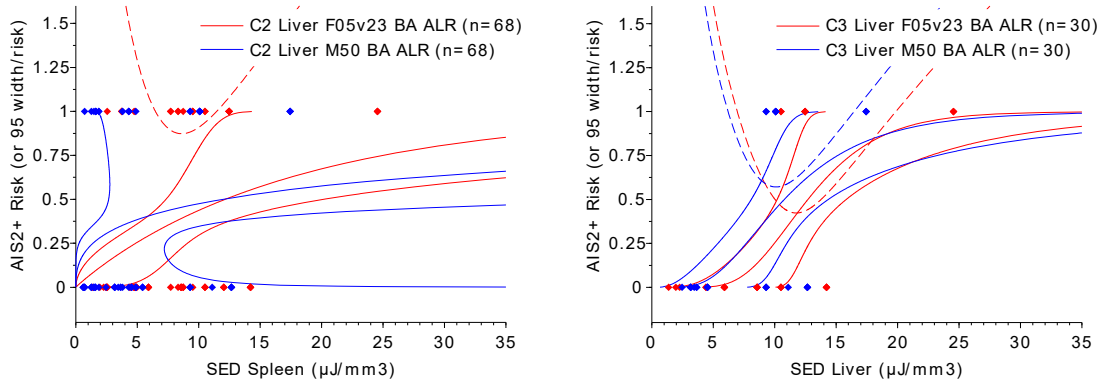

Fig. 7. M50 vs. F05 C2 (left) vs. C3 (right) risk curves (all configurations used) comparison illustrating the reduction of the difference between models with the C3 selection. Legends as in Fig. 3.

IV. DISCUSSION

Different liver and spleen AIS2+ injury risk curves were built for two models of the GHBMC family using different model scaling assumptions and selections of loading configurations.

While global model scaling to match the height, weight and relevant abdominal depth of PMHSs predicted based on anthropometric regressions was found in [7] to explain some of the variance in the response, e.g., for displacement metrics, scaling had almost no effect on the injury prediction (based on the paired simulation for 57 PMHSs). Many causes could possibly contribute to this result including:

(1) the scaling does not account for the internal structures, and the scaling of the organs (following the external dimensions) may not capture actual correlations with anthropometric dimensions,

(2) the choice of metric (density) may have the effect of normalising the criteria independently from the size,

(3) many setups are focused on a single anatomical region, e.g., impactor regional loading, and the effect of stature and mass scaling may be limited on the tissue response,

(4) the tolerance is not related to scaled parameters.

Improved scaling better accounting for internal anatomical structures may help but it would not account for specimen-to-specimen variations as information about internal organ geometry are limited in past PMHS studies. Additional scaling limitations include the absence of scaling for material properties, including both stiffness and tolerance values, for both soft and skeletal structures. Besides scaling, other parameters that may have affected the results include the initial posture, or the sensitivity to small variations of stimulus or impact location. While posture was for example found to affect the response of the THUMS model [18], it was not adjusted in the current study. This may not have been critical for some of the configurations using impactors directly focused on the organs of interest (e.g. Kremer oblique impact, [14]) and for which the body moves very little prior to peak compression. This may be more important for side impact configurations with more body kinematics (e.g. Cavanaugh side impact sled [9]). This may have been mitigated by the fact that the forces transmitted to the abdomen plate were checked (Appendix) but should be further investigated. The sensitivity to stimulus or impact location variations was not studied specifically. The use of an average stimulus for baseline models may have introduced a bias in the baseline to scaled paired comparisons and in the injury predictions. This could be addressed in the future by performing all M50 and F05 baseline simulations with exact stimuli corresponding to all PMHS (68 PMHS times two models). Regarding the sensitivity to small variations of impact location, no large change in SED were found for small changes of impactor height in [2], suggesting that considering only large variations of impact location (C2 vs C3) could have significant effects. This could however be checked by performing sensitivity analyses for other impact configurations. For the moment, scaling as performed for the current study did not appear to bring additional value compared to baseline runs for the generation of risk curves. Baseline runs, which were considerable less costly in terms of model preparation and could be less costly for future updates, were therefore used.

Large risk differences were observed between M50 and F05 when using all setups (C2). These are in line with previous observations [2][7] related to organ engagement and SED differences between F05 and M50. In practice, some simulations with limited organ engagement (M50 liver in particular) correspond to injurious tests, e.g., Hardy bar mid abdomen, leading to risk curves with unacceptable rating and wide confidence intervals in the low energy range. The F05 liver position mitigates this effect, giving the impression that the F05 better predicts injuries despite its modelling similarity to the M50. The risk curves ratings are widely improved and the differences between models reduced when organ engagement is controlled (C3). The liver risk curves rating becomes good for the F05 (or nearly good for the M50). The improvement is limited for the spleen, but this can be attributed to the limited number of injury in the sample (only four in the C3).

These observations have multiple implications. First, they suggest that the liver and spleen positions are critical to determine the injury risk with human models. As the positions are unknown in most PMHS tests, many tests from the literature may be poorly suited to determine the injury tolerance using a model vs. test matching approach, as in the current study. In the short term, literature datasets that have not been used yet, e.g., [19], should be examined to see if they are suitable to improve the prediction capability. In the longer term, it is hoped that more suitable experimental data can be collected, i.e., that better documents the relative positions of organ and impacting surface (in the test position), or that uses loading surfaces engaging organs with certainty. In that context, targeting the spleen (and kidneys) could be of particular interest as very few suitable tests were found

for these organs and that there is hope (at least for the spleen) to develop risk curves with a few more data points.

Second, the observations raise questions about the meaning of risk curves for a single model, i.e., with a specific organ geometry. The C3 curves may represent reasonably well (cf. rating) the risk of liver injury for the specific organ geometry of the F05 and M50, and perhaps other organ geometry, for loading directly onto the upper abdomen region. However, for loading to the mid-abdomen, the two models (F05 and M50) would lead to different predictions. It is unknown if the F05 over predicts mid-abdomen risk or if the M50 under predicts as it may depend how representative these models are for that region. Also, while the M50 and F05 are based on living human subjects imaged in a seated position [20], it is unclear if the PMHSs are representative of live humans in that region or if there could have been some caudal motion of the liver and diaphragm in relation to the absence of muscle tone or other parameters (cf. [6]). It is noteworthy to observe that Hardy and Cavanaugh mid-abdomen bar impacts are in close locations and lead to similar external responses [13], but have very different injury outcome. Overall, the effect of the statistical distribution of organ location in the population on the injury risk for different impact locations should be further investigated. For now, the C3 curves should be used cautiously for impact locations away from the organs and the C2 and even C1 results may help provide a more conservative assessment for mid-abdomen loading. It also needs to be remembered that the risk curves are model based, i.e,. model dependent. They should not be used with other models although the methodology could be used with other models to develop similar risk curves. As the risk curves depend on the simulation performed, they should be updated or at least verified when modelling parameters are changed, including with model versions. Also, the risk curves are expected to be sensitive to the choice of material properties for the solid organs. At this point, it is unknown how changes in stiffness or non-linearity would affect the risk curves and their confidence interval. In some cases, only the scale on the abscissa may be affected or in others, the confidence intervals may be widened or reduced. This sensitivity should be studied in the future. Also, the choice of injury criterion should be further investigated as some criteria (e.g. purely strain based) may be less sensitive to stiffness variations than the current strain energy density approach.

Several other limitations and perspectives can be mentioned. First, only one injury criterion was tested. Other criteria, including more local criteria, e.g., SED or strain in a region of the organ, could be checked to see if a better predictor can be found based on the same dataset. A more local criterion may also help with respect to the sensitivity of the outcome to the relative position of the organ and impactor. Another limitation is the sensitivity of the results to the experimental studies, and the need for objective criteria to select the studies. Besides the case of Hardy and Cavanaugh mid-abdomen bar impacts giving different injury outcomes for similar loading, Kremer and Viano oblique impacts, which are both included in the C3 sample, have opposite injury outcomes. Removing any of them affects the risk curve, e.g., Fig. 8 for the M50, but improves the curve rating in both cases. In the absence of objective reasons to remove one of them, both were kept, but it is hoped that loading conditions can be added to reduce the sensitivity to specific studies, and perhaps be able to remove outliers.

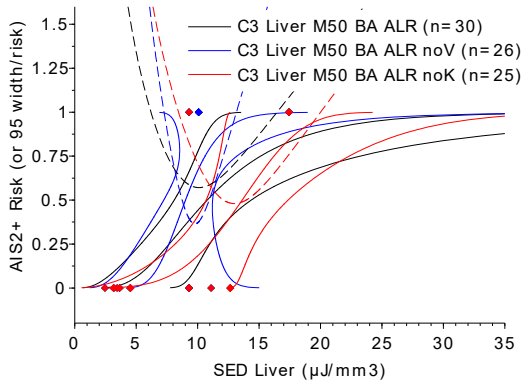

Fig. 8. C3 M50 Liver risk curve: effect of Viano (noV) or Kremer Oblique (noK) removal. Legends as in Fig. 3.

V. CONCLUSIONS

Model based injury risk curves were developed for the liver and spleen of the GHBMC M50 and F05 models. A good or fair injury prediction capability (using ISO rating) was attained for the liver when selecting carefully the

loading condition based on the organ engagement. No equivalent result could be obtained on the spleen, most likely due to the insufficient number of injury points. The study highlights the critical importance of organ geometry and loading location to predict injury, and these parameters should be considered when using the risk curves to predict injury (especially for mid-abdomen impact). The effect of organ geometrical distribution will be investigated in the future to better estimate the risk in the whole population in that region.

VI. ACKNOWLEDGEMENT

The Global Human Body Models Consortium, LLC (GHBMC), provided funding for this study. The views expressed in this paper are those of the authors and do not necessarily represent those of the GHBMC.

VII. REFERENCES

[1] Helfenstein, C, Gennisson, J-L, Tanter, M, Beillas, P. (2015) Effects of pressure on the shear modulus, mass and thickness of the perfused porcine kidney. *Journal of Biomechanics*, **48**(1): pp.30–37.

[2] Le Ruyet, A, Berthet, F, Rongiéras, F, Beillas, P. (2016) Effect of Abdominal Loading Location on Liver Motion: Experimental Assessment using Ultrafast Ultrasound Imaging and Simulation with a Human Body Model. *Stapp Car Crash Journal*, **60**: pp.25–57.

[3] Beillas, P, Lafon, Y, Smith, FW. (2009) The effects of posture and subject-to-subject variations on the position, shape and volume of abdominal and thoracic organs. *Stapp Car Crash Journal,* **53**: pp.127–154.

[4] Hayes, AR, Gayzik, FS, Moreno, DP, Martin, RS, Stitzel, JD. (2013) Abdominal Organ Location, Morphology, and Rib Coverage for the 5th, 50th, and 95th Percentile Males and Females in the Supine and Seated Posture using Multi-Modality Imaging. *Annals of Advances in Automotive Medicine*. **57**: pp.111–122.

[5] Parenteau, CS, Ehrlich, P, Ma, L, Su, GL, Holcombe, S, Wang, SC. (2013) The quantification of liver anatomical changes and assessment of occupant liver injury patterns. *Stapp Car Crash Journal,* **57**: pp.267–283.

[6] Howes, MK, Hardy, WN, Beillas, P. (2013) The effects of cadaver orientation on the relative position of the abdominal organs. *Annals of Advances in Automotive Medicine*, **57**: pp.209–224.

[7] Beillas, P, Berthet, F. (2017) An investigation of human body model morphing for the assessment of abdomen responses to impact against a population of test subjects. *Traffic Injury Prevention*, **18**(sup1): pp.S142–S147.

[8] Snedeker JG, Barbezat M, Niederer P, Schmidlin FR, Farshad M. (2005) Strain energy density as a rupture criterion for the kidney: impact tests on porcine organs, finite element simulation, and a baseline comparison between human and porcine tissues. Journal Biomechanics, **38**(5): pp.993–1001.

[9] Cavanaugh, JM, Walilko, T, Chung, J, King, AI. (1996) Abdominal injury and response in side impact. *Proceedings of the Stapp Car Crash Conference*, pp.1-16

[10] Cavanaugh, JM, Nyquist, GW, Goldberg, SJ, King, AI.(1986) Lower abdominal tolerance and response. *Proceedings of the 30th Stapp Car Crash Conference*, pp.41-63.

[11] Foster, CD, Hardy, WN, Yang, KH, King, AI, Hashimoto, S. (2006) High-speed seatbelt pretensioner loading of the abdomen. *Stapp Car Crash Journal*, **50**: pp.27-51.

[12] Hallman JJ, Yoganandan N, Pintar FA. (2010) Biomechanical and injury response to posterolateral loading from torso side airbags. *Stapp Car Crash Journal*, **54**: pp.227-57.

[13] Hardy, WN, Schneider, LW, Rouhana, SW. (2001) Abdominal impact response to rigid-bar, seatbelt, and airbag loading. *Stapp Car Crash Journal*, **45**: pp.1-31

[14] Kremer, MA, Gustafson, HM, Bolte, JH, Stammen J, Donnelly B. (2011) Pressure-based abdominal injury criteria using isolated liver and full-body post-mortem human subject impact test. *Stapp Car Crash Journal*, **55**: pp.317-350.

[15] Lamielle, S, Vezin, P, Verriest, JP, Petit, P, Trosseille, X, Vallancien, G. (2008) 3D deformation and dynamics of the human cadaver abdomen under seatbelt loading. *Stapp Car Crash Journal*, **52**: pp.267-294.

[16] Viano, DC, Lau, IV, Asbury, C, King, AI, Begeman, PC. (1989) Biomechanics of the human chest, abdomen, and pelvis in lateral impact. *Proceedings of the 33rd Annual Meeting of the Association for the Advancement of Automotive Medicine*, pp.367-382.

[17] ISO TS18506. Procedure to construct injury risk curves for the evaluation of occupant protection in crash tests Related Electronic Documents. Internet: http://standards.iso.org/iso/18506 [cited 2018, June 5th]

[18] Poulard, D, Subit, D, Nie, B, Donlon, J-P, Kent, RW. (2015) The Contribution of Pre-impact Posture on Restrained Occupant Finite Element Model Response in Frontal Impact. Traffic Injury Prevention.**16** Suppl 2: pp.87-95.

[19] Ramachandra, R, Kang, YS, et al. (2016) Biomechanical Responses of PMHS Subjected to Abdominal Seatbelt Loading. *Stapp Car Crash Journal,* **60**: pp.59–87.

[20] Gayzik, FS, Moreno, DP, Geer, CP, Wuertzer, SD, Martin, RS, Stitzel, JD. (2011) Development of a full body CAD dataset for computational modeling: a multi-modality approach. *Annals of Biomedical Engineering,* **39**(10): pp.2568–2583.

VIII. APPENDIX

Appendix A – GHBMC model response in the Cavanaugh sled setup [9].

The setups with soft and hard padding were selected from [9] for the simulation matrix. The sled plates were modelled using the description in the original study. Their positions were adjusted such that they engaged the target anatomical region, e.g., thorax for the thorax plate. The padding properties (paper honeycomb) was modelled using a MAT_MODIFIED_HONEYCOMB material law. Material parameters (stresses and modulus) were scaled from a LSTC barrier example to the static crush strength provided in [9] adjusted to account for the strain rate effect. A factor 1.8 was selected for the effect of strain rate based on [A1]. Two scenarios were considered to account for possible differences in arm posture between the model and the PMHS: (1) the arm engaged the thorax and abdomen plate or (2) no contact was defined between the two.

An illustration of the response is provided in Fig. A-1 below for the F05 model and the stiff padding. For the abdomen force, the effect of the arm contact was limited on the F05 and more prominent on the M50. Fig. A-1 also illustrates the organ involvement on the abdomen plate (liver in blue, spleen in red). The average of the SED obtained in the two contact hypotheses was used.

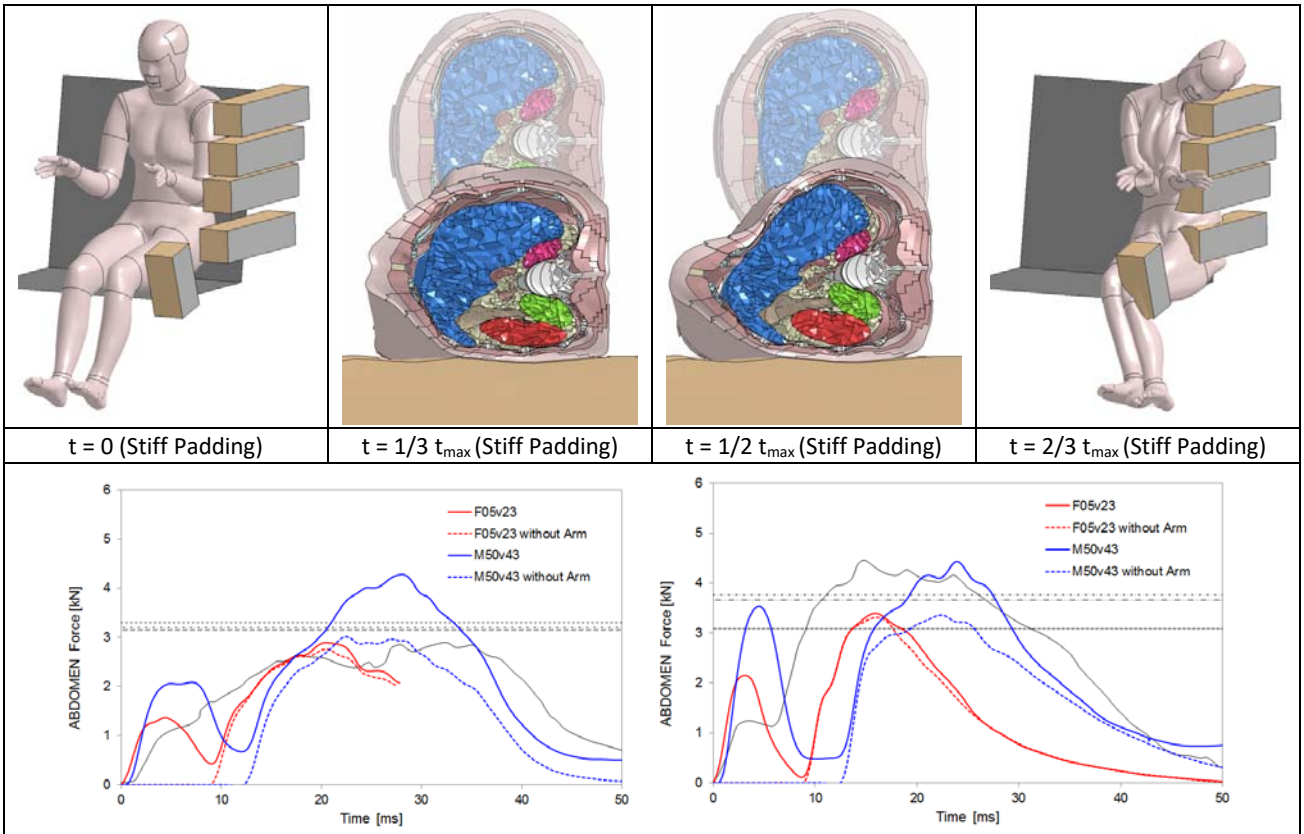

Fig. A-1. Illustration of the response for the Cavanaugh sled simulation.

IX. APPENDIX REFERENCES

[A1] Wang, Z-W., E, Y-P. (2011) Energy-Absorbing Properties of Paper Honeycombs under Low and Intermediate Strain Rates. *Packaging Technology and Science,* 2012; 25: pp.173–185.